Interactions between Stationary Planetary Waves in the Stratosphere

WALTER A. ROBINSON

Department of Atmospheric Sciences, University of Washington, Seattle, WA 98195

(Manuscript received 6 August 1985, in final form 26 December 1985)

ABSTRACT

Interactions between stationary planetary waves are investigated in the context of severely truncated quasi-geostrophic dynamics in a midlatitude beta-channel. Such interactions are solely a consequence of dissipation and are mediated by waves with smaller meridional scales. Linear numerical experiments with wave 1 and 2 basic states indicate that wave 1 is amplified in a wave 2 basic state, while the behavior of a wave 2 disturbance in a wave 1 basic state is sensitive to the relative phases of the waves. At some phases, wave 2 is confined below the region of large wave 1 amplitudes.

The dynamics of these interactions are diagnosed using the potential enstrophy budgets of the waves. These budgets are more sensitive to the wave–wave interactions than are the amplitudes of the waves themselves. Nonlinear experiments show behavior that is a combination of the linear results with an amplification of wave 1 and a strong dependence on the relative phases of waves 1 and 2 in the stratosphere.

1. Introduction

Since the appearance of Charney and Drazin's seminal paper in 1961, linear theory has often been applied to describe the structures of stationary disturbances in the extratropical stratosphere. Charney and Drazin used the dispersion relation for three-dimensional Rossby waves to explain the confinement of stationary waves beneath the strongest stratospheric westerlies. Matsuno (1970) extended Charney and Drazin's results to spherical geometry and demonstrated the importance of the refractive index for planetary waves. Simmons (1974) studied the behavior of stationary waves in a beta-channel. His results emphasized the importance of the meridional curvature of the zonal wind and showed that the strongest wave amplitudes are channeled into the center of the polar night jet. Subsequent studies by Schoeberl and Geller (1974) using the quasi-geostrophic system and Lin (1982) using primitive equations have confirmed the sensitivity of the wave structures to the details of the zonal wind profile and have shown that the waves can be modified significantly by dissipation.

These linear studies have done well in reproducing the structures of stationary planetary waves. Because the results are sensitive to the zonal winds and the rates of dissipation, it is not generally necessary to call upon nonlinear effects to explain discrepancies between observations and the modeled structures of stationary planetary waves. Yet situations exist in which wave–wave interactions may be important in determining the time-averaged flow. Such a case was recently elucidated by Austin and Palmer (1984). Using a primitive equation model of the stratosphere they showed that interactions with other waves were necessary in order to explain the large amplitude of wave 1 and its lack of upward propagation across the tropopause during December 1980.

Another suggestion that interactions between stratospheric stationary waves may be important comes from Labitzke's (1977) analysis of planetary wave amplitudes at 30 mb during twelve Northern Hemisphere winters. These data reveal a tendency for the amplitudes of waves 1 and 2 to be anticorrelated on time scales of a month or longer. [This is distinct from the anticorrelation of the waves on weekly timescales, the so-called wave 1–wave 2 vacillation (Smith et al., 1984).] Periods of weaker-than-normal wave 2 (December 1965, December 1969/January 1970) are associated with larger-than-normal amplitudes of wave 1.

The present study is an investigation of the interactions between stationary planetary waves 1 and 2 using the simplest model that allows such interactions, a severely truncated quasi-geostrophic model in a midlatitude beta channel. In this model all wave–wave interactions are a consequence of dissipation. Section 2 discusses the theory of dissipation-induced interactions, treating interactions between weak waves under the severe truncation. The small amplitude results are no longer valid when the potential vorticity of the waves is of the same order as that of the mean flow, and different behavior is expected under this condition.

Section 3 describes the numerical model used in this study and the method by which the model equations are solved. Section 4 presents results for small amplitude wave 1 in a basic state, which includes finite amplitude wave 2, and for small amplitude wave 2 in a

wave 1 basic state. Results for waves 1 and 2, both possessing finite amplitudes, are presented in section 5. The final section summarizes the results and discusses their relevance to the atmosphere.

2. Theory

We consider the behavior of midlatitude stationary disturbances confined to the polar night jet by its strong meridional gradient of potential vorticity. Such waves are well represented in quasi-geostrophic beta-plane dynamics. The flow is governed by the conservation of the quasi-geostrophic potential vorticity (PV), q, following the geostrophic flow:

$$J(\psi, q) = S, \tag{1}$$

where J is the horizontal Jacobian, ψ the geostrophic streamfunction and q is given by

$$q = \beta y + \nabla^2\psi + \frac{\partial}{\partial z}(\rho_0 \epsilon \psi_z)/\rho_0,$$

where β is the meridional gradient of the planetary vorticity, y the meridional coordinate, ρ_0 the basic state density, ϵ the stability parameter ($\epsilon = f_0^2/N^2$ where N is the Brunt–Väisälä frequency), z a log-pressure vertical coordinate [$z = H \ln(P_0/P)$ where P is the pressure], P_0 a reference pressure and H is the density scale height, taken equal to 7 km, and S represents a source of PV. In the present study we are concerned with interactions between zonally asymmetric modes, as opposed to interactions between the waves and the zonal mean flow. The basic state zonal flow is held fixed and Eq. (1) becomes

$$\bar{u}q'_x + \bar{q}_y\psi'_x + J(\psi', q') = S'. \tag{2}$$

Consider two waves, each of which satisfies the linear equation

$$\bar{u}q'_{nx} + \bar{q}_y\psi'_{nx} = S'_n, \quad n = 1, 2. \tag{3}$$

The waves are assumed to be of the form

$$\begin{pmatrix}\psi'_n \\ q'_n\end{pmatrix} = \mathrm{Re}\left[\begin{pmatrix}\psi_n \\ q_n\end{pmatrix} e^{ik_n x} \sin l_n y\right], \tag{4}$$

where

$$q_n = -K_n^2\psi_n + \frac{1}{\rho_0}\frac{\partial}{\partial z}(\rho_0\epsilon\psi_{nz}),$$

$$K_n^2 = k_n^2 + l_n^2.$$

The source term, S, is parameterized as constant rates of Newtonian cooling and Rayleigh friction

$$S_n = -D_N q_n - K_n^2(D_N - D_R)\psi_n, \tag{5}$$

where D_N and D_R are, respectively, the rates of Newtonian cooling and Rayleigh friction. The PV of each mode is related to its streamfunction by

$$q_n = -\frac{\psi_n}{(1 + d_N^2)}\{\bar{\alpha} - K_n^2 d_N(d_R - d_N) + i[d_N\bar{\alpha} + K_n^2(d_R - d_N)]\}, \tag{6}$$

where

$$\bar{\alpha} = \bar{q}_y/\bar{u},$$

$$d_N = \frac{D_N}{k_n\bar{u}}, \quad d_R = \frac{D_R}{k_n\bar{u}}.$$

For long waves in the polar night jet, both d_N and d_R are small, O(1/10), and to first order in the dissipation

$$q_n = -\psi_n\{\bar{\alpha} + i[d_N\bar{\alpha} + K_n^2(d_R - d_N)]\}. \tag{7}$$

The PV of each wave has two components: one denoted q_R, in phase with the streamfunction, and the other q_I, 90° out of phase with the streamfunction. The interaction between the waves is given by

$$J(\psi'_1, q'_2) + J(\psi'_2, q'_1) = \bar{\alpha}_y[\psi'_{1x}\psi'_2 + \psi'_{2x}\psi'_1] + J(\psi'_1, q'_{2I}) + J(\psi'_2, q'_{1I}). \tag{8}$$

The first term vanishes if $\bar{\alpha}$ does not vary with latitude. That this is approximately true for the Northern Hemisphere midlatitude stratosphere was shown by Derome (1984). He pointed out that under this condition, and in the absence of dissipation, an arbitrary stationary solution of the linear PV equation is a solution of the fully nonlinear equation. This is consistent with the success of linear theory in the stratosphere where the observed stationary disturbances have large amplitudes.

For $\bar{\alpha}$ which varies only with altitude, stationary wave–wave interactions occur primarily because dissipation induces a component of the PV of each wave which is in quadrature with its streamfunction. In a positive meridional gradient of PV, waves typically transport PV southward (down gradient). This requires a positive value for q_I, i.e., q_I is $\frac{1}{4}$ wavelength to the east of the geopotential ridge.

The interaction between two planetary waves forces additional waves whose wavenumbers are the sums and differences of the wavenumbers of the primary waves. In a beta-channel a mode can be defined by its zonal and meridional wavenumbers, m and n, and its zonal phase Θ.

$$\psi'_{mn} \sim \cos(mkx + \Theta)\sin\frac{n\pi y}{L}, \quad 0 \leqslant y \leqslant L \tag{9}$$

where k is the gravest zonal wavenumber for a zonally cyclic channel, and L is the meridional width of the channel. For present purposes we consider only primary waves for which $m = 1$ or 2, and for which $n = 1$.

The interaction between two waves with the same meridional scale gives rise to two modes. In particular the interaction $J(A, B)$ where

$$A = a\cos(kx + \Theta_A)\sin\frac{\pi y}{L},$$

and

$$B = b\cos(2kx + \Theta_B)\sin\frac{\pi y}{L}$$

is given by

$$J(A, B) = \frac{ab}{4}\frac{k\pi}{L}\sin\frac{2\pi y}{L} \times [3\cos(kx + \Theta_B - \Theta_A - 90°) + \cos(3kx + \Theta_A + \Theta_B - 90°)]. \quad (10)$$

The interaction of waves 1 and 2 forces the second meridional modes of waves 1 and 3 (denoted 1′ and 3′). The forcing of wave 1′ is three times stronger than that of wave 3′. Thus the effect on waves 1 and 2 of their interaction is primarily governed by the strength and phase of wave 1′. Because of its small horizontal scale, this wave has much more PV associated with a given geopotential amplitude than either wave 1 or 2, so that the interactions of waves 1 and 2 with wave 1′ are dominated by their advection of its PV.

The potential vorticity equation for wave 1′ is

$$ik[\bar{u}q(1') + \bar{q}_y\psi(1')] = F + D, \quad (11)$$

where D is the dissipation of this mode and F is its nonlinear forcing. If both waves 1 and 2 are extracting PV from the zonal flow so that q_I is positive for both waves, then the phase of the PV forcing for wave 1′ is given by

$$\Theta_F(1') = \Theta_\psi(2) - \Theta_\psi(1). \quad (12)$$

The phase of the forcing of wave 1 by the wave 2 advection of wave 1′ PV is

$$\Theta_F(1) = -\Theta_q(1') + \Theta_\psi(2) + 90°, \quad (13a)$$

and for wave 2

$$\Theta_F(2) = \Theta_q(1') + \Theta_\psi(1) - 90°. \quad (13b)$$

Forcing reinforces a wave when the forcing coincides with the wave's PV, i.e., $\Theta_F = \Theta_q$ or $\Theta_F \approx \Theta_\psi + 180$. The phase of a wave is set by the phase of its forcing and the phase lag of its response to that forcing

$$\Theta_q = \Theta_F + \Theta_R. \quad (14)$$

Combining Eqs. (12) and (14) with (13a) and (13b) yields

$$\Theta_F(1) = -\Theta_q(1') + \Theta_\psi(2) + 90° = \Theta_\psi(1) - \Theta_R(1') + 90°, \quad (15a)$$

and

$$\Theta_F(2) = \Theta_\psi(2) + \Theta_R(1') + 90°. \quad (15b)$$

Whether wave 1 or wave 2 is reinforced by their interaction depends on $\Theta_R(1')$. If the amplitude of waves 1 and 2 and thus the strength of the nonlinear forcing of wave 1′ vary smoothly with height, then the PV of this wave with its small horizontal scale will be dominated by its barotropic component,

$$q(1') \approx -K^2(1')\psi(1'),$$

and the inviscid PV equation for wave 1′ is approximately

$$q(1') = \frac{-iF}{k\bar{u}\{1 - \bar{q}_y/[\bar{u}K^2(1')]\}},$$

where F is the nonlinear forcing. In the strong stratospheric westerlies, K^2 for wave 1′ should be much larger than $\bar{q}_y/\bar{u}$, and $\Theta_R(1')$ will tend toward −90°. Thus, for waves 1 and 2, which are interacting sufficiently weakly so that their linear structures are approximately maintained, their dissipation-induced interaction proceeds through wave 1′ so as to reinforce wave 1 and erode wave 2. This behavior is displayed in the numerical results presented in section 4.

When the amplitudes of the waves are large the results of the preceding paragraphs are no longer valid. Consider a basic state consisting of a zonal flow and a single wave of sufficiently large amplitude that there are regions of closed streamlines. In these regions are points where the flow and the PV gradient of the basic state vanish. In the presence of dissipation a perturbation to this basic state must balance its dissipative loss of PV against the basic state advection of its PV and the perturbation advection of the PV of the basic state. Both of these terms go to zero at the center of the region of closed streamlines, and the perturbation PV must also vanish at this point. Results presented in section 4 show this exclusion of a wave 2 perturbation from the regions of weak flow in a basic state that is distorted by wave 1.

3. Description of the model

The present model includes eight interacting horizontal modes with three zonal wavenumbers and two meridional scales in a quasi-geostrophic beta-channel, 40 deg wide. The streamfunction is given by

$$\psi = \sum_{n=1}^{2}\{\psi_n\cos(n\pi y/L) + \mathrm{Re}[\sum_{m=1}^{3}\psi_{mn}e^{imkx}\sin(n\pi y/L)]\}, \quad (16)$$

where the subscripted coefficients are functions of height. Here L is the width of the channel, and k is the gravest zonal wavenumber $k = (a\cos 60°)^{-1}$ where a is the radius of the earth. The quasi-geostrophic PV equation is solved at 50 levels extending from the surface to 122.5 km. The streamfunction for each mode is found by inverting the expression for its PV.

Steady solutions of the model equations are found by iteration. The linear structures for each wave are computed. Then the wave–wave interactions are eval-

uated and applied as forcing for the recalculation of the wave structures. The gravest zonally symmetric mode ($n = 1$), subsequently referred to as the mean flow, is held fixed. For large wave amplitudes it is found that the iteration sometimes diverges, so a filtered iteration is employed. At step j

$$\left.\begin{aligned} Z\hat{\psi}^j &= F^j \\ \psi^{j+1} &= (1-f)\hat{\psi}^j + f\psi^j \end{aligned}\right\}, \tag{17}$$

where Z is the operator comprising all of the linear terms in the PV equation for a mode; F^j is the wave–wave forcing of the mode computed from the wave amplitudes at step j, and f is the underrelaxation parameter. For some experiments values of f as large as 0.9 are required for convergence. The iteration is continued until subsequent steps yield identical wave amplitudes and phases to five digits.

The model's "physics" are entirely linear, allowing all wave–wave interactions to be ascribed to the dynamics. Dissipation comprises Newtonian cooling and Rayleigh friction. Rates for the former process are those used by Holton and Mass (1976), and rates of Rayleigh friction are taken from Holton and Wehrbein (1980). These profiles are shown in Fig. 1.

Dissipation moves the flow toward a zonally symmetric basic state, which resembles a Northern Hemisphere January. This basic state is obtained by computing the meridional gradient of PV associated with the winds shown in Fig. 2a. To be consistent with the model truncation, both these winds and their associated gradient of PV are separately projected onto $\sin(\pi y/L)$. The resulting winds are shown in Fig. 2b.

Because we are interested in the effects of stratospheric wave–wave interactions, the waves are subject

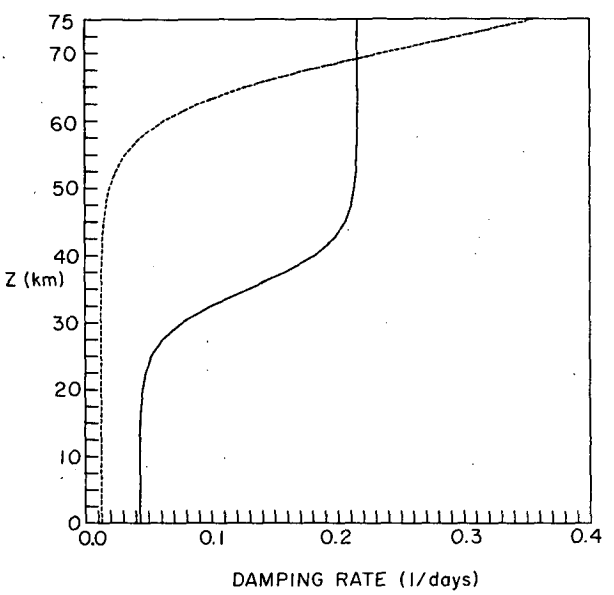

FIG. 1. Dissipation rates used in the model (days^{-1}): Newtonian cooling (solid) and Rayleigh friction (dashes).

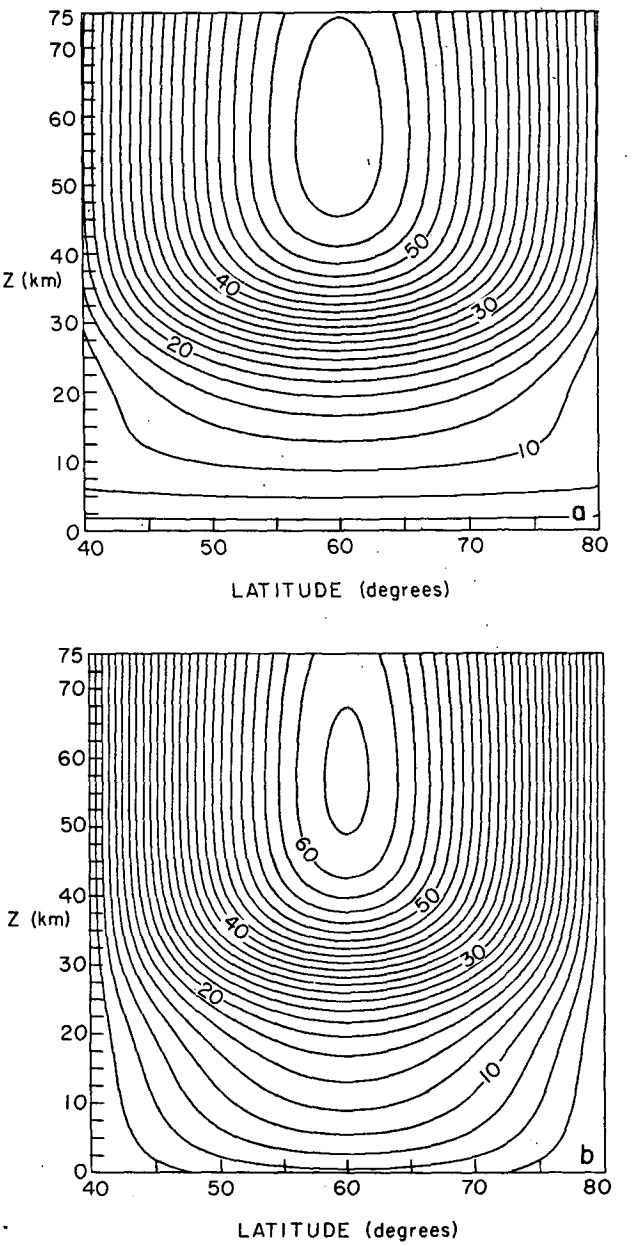

FIG. 2. Zonal wind profiles (m s^{-1}) for the model: (a) basic state used to compute the zonally symmetric potential vorticity and (b) projection of this profile onto $\sin\pi y/L$.

to a fixed forcing from the lower boundary of the model, and the surface boundary condition is linearized. The appropriate boundary condition for the PV equation with a log-pressure vertical coordinate has been derived by Tung (1983). For our present purposes this condition can be written

$$\bar{u}\delta'_x + \bar{\delta}_y\psi'_x = -f_0(w_E + w_F) - \epsilon D_N\psi'_z \quad (z = 0), \tag{18a}$$

where

$$\delta' = \epsilon\left(\psi'_z - \frac{N^2}{g}\psi'\right). \tag{18b}$$

For application to the model, $\bar{X}$ refers to the X amplitude of the gravest zonally symmetric mode, and X' refers to any other mode; w_F is the forcing applied at the surface to generate the wave, and w_E is the vertical velocity induced by Ekman suction at the top of the planetary boundary layer

$$w_E = D_E \nabla^2 \psi' \quad (z = 0), \tag{19}$$

where D_E is a depth equal to 150 m.

4. Linear experiments

For the experiments discussed in this section the model is linearized around a zonally asymmetric basic state that includes a finite amplitude wave 1 or wave 2. We investigate the behavior of a small amplitude wave 2 or wave 1 disturbance in these basic states. The linear structures of waves 1 and 2 in the zonally symmetric basic state are shown in Fig. 3a, b. These structures are roughly consistent with observations (van Loon et al., 1973).

a. Wave 1 in a wave 2 basic state

For a small amplitude wave 1 in a wave 2 basic state only modes 1′, 3, and 3′ are generated. Wave 1 is amplified by its interaction with wave 2, as is anticipated from the discussion in section 2. Figure 4a shows the amplitudes of wave 1 in basic states that include wave 2 with amplitudes of 0, 250, 500 and 750 m at 32.5 km. The amplitude of wave 1 increases with the strength of wave 2 for wave 2 amplitudes less than 500 m. When the amplitude of wave 2 is increased past 500 m the response of wave 1 is reduced. (The reason for this saturation is discussed below.) The corresponding phases of wave 1 are shown in Fig. 4b. As the strength of wave 2 is increased, the westward slope of wave 1 decreases. For a wave 2 amplitude of 750 m, wave 1 slopes eastward with height across the tropopause, an indication of downward propagation.

The dynamics of this behavior are best understood in terms of the potential enstrophy budget for wave 1. The PE budget for a wave indicates the relative importance of wave–wave interactions, wave–mean flow interactions, and dissipation in maintaining the wave (Smith, 1983). Consider the PV equation for a stationary wave subject to forcing, F', by wave–wave interactions and to (for simplicity) equal rates, D, of Newtonian cooling and Rayleigh friction.

$$Dq' + \bar{u}q'_x + \bar{q}_y\psi'_x = F'. \tag{20}$$

An equation for the PE is obtained by multiplying (20) by q' and zonally averaging, giving

$$Q_D + Q_{MF} + Q_{WW} = 0, \tag{21}$$

where

$$Q_D = -2DQ,$$

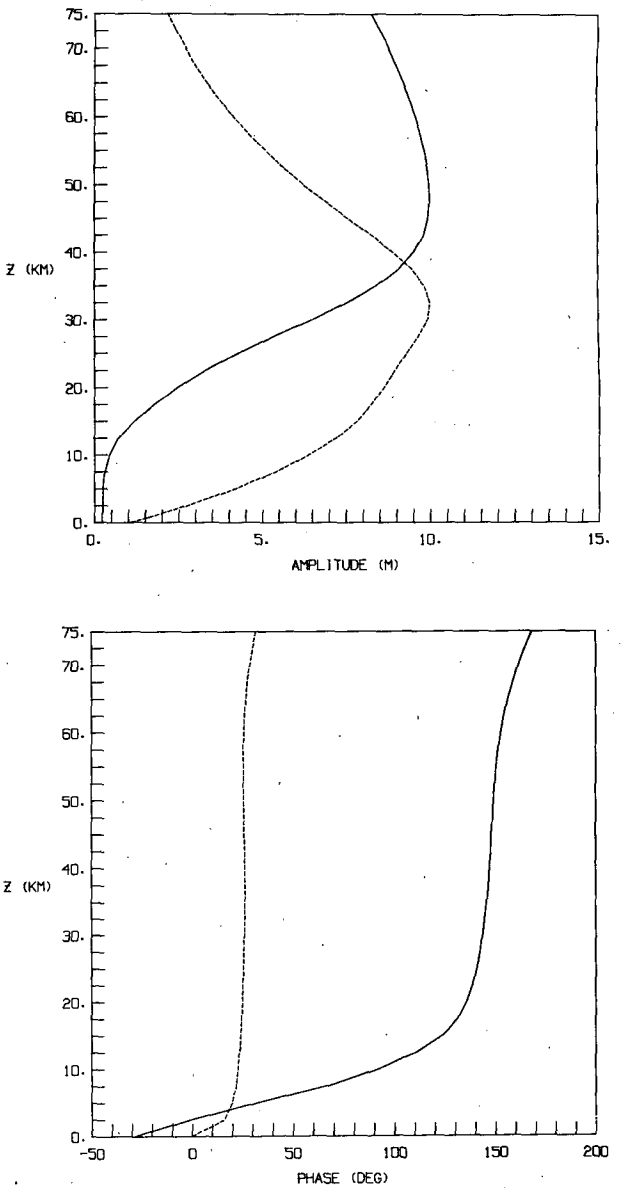

FIG. 3. (a) Amplitudes (arbitrary units) and (b) phases (deg) of waves 1 and 2 in the zonally symmetric basic state.

$$Q_{MF} = -\bar{q}_y\overline{q'\psi'_x}$$

$$Q_{WW} = \overline{q'F'}$$

and

$$Q = \frac{1}{2}\frac{1}{\overline{q'^2}}.$$

Equation (21) states the balance that must be satisfied by any stationary disturbance; Q_D is the rate at which PE is gained by dissipation (Q_D is usually negative), Q_{WW} is the rate at which PE is gained from other waves, and Q_{MF} is the rate at which the wave extracts PE from the mean flow.

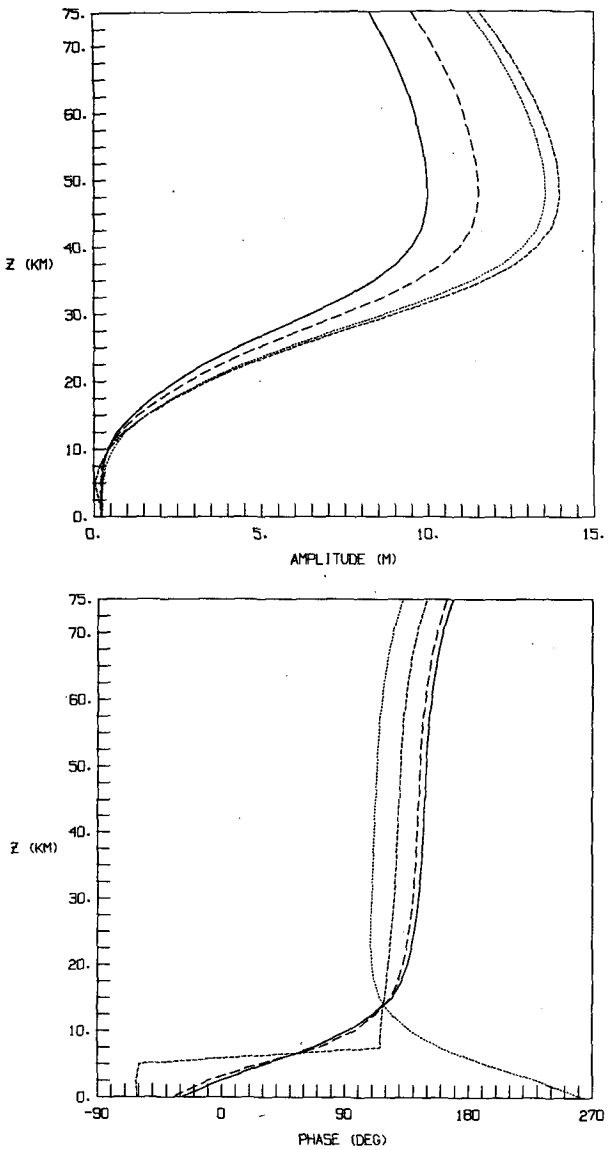

FIG. 4. (a) Amplitudes and (b) phases of wave 1 in wave 2 basic states. The curves correspond to wave 2 amplitudes at $z = 32.5$ km of 0 (solid), 250 (long dashes), 500 (short dashes), and 750 m (dots).

The PE budgets for wave 1 in the wave 2 basic states are shown in Fig. 5. Here Q_{WW} and Q_{MF} are shown along with Q_{MF} for the wave in a zonally symmetric basic state. The values are weighted by the density so that the figures are not dominated by large but energetically insignificant values associated with the rapid dissipation above 70 km. In a zonally symmetric basic state Q_{MF} is exactly balanced by Q_D; Q_{MF} is large in the stratosphere where wave 1 is strong and also in the troposphere where the weak zonal winds lead to very effective dissipation. For a moderate amplitude of wave 2 (Fig. 5a), wave–wave interactions make a modest contribution to the PE of wave 1 in the troposphere and lower stratosphere, and there is a compensating decrease in Q_{MF}. When the amplitude of wave 2 is increased (Fig. 5b, c) the region of strong wave–wave reinforcement of wave 1 extends upward and its magnitude increases. The Q_{MF} compensates by decreasing and becoming negative in the troposphere and lower stratosphere. Because of this compensation the amplitude of wave 1 is less sensitive to the amplitude of wave 2 than is its PE budget.

Why does wave 1 respond to increased wave–wave forcing by returning PE to the zonal flow rather than by increasing in amplitude? This can be understood if we recognize that the wave–wave forcing is not externally imposed. Rather, it is a positive feedback for wave 1 which depends on the generation of wave 1′ by the interaction of waves 1 and 2. For purposes of argument this feedback is parameterized as being linear, i.e.,

$$Q_{WW} = 2\lambda Q, \tag{22}$$

with the magnitude of λ increasing with the strength of wave 2. The PE equation for wave 1 becomes

$$2(D - \lambda)Q = Q_{MF}. \tag{23}$$

As the amplitude of wave 2 and thus the value of λ is increased, the wave–wave feedback effectively reduces the dissipation, and the amplitude of wave 1 increases. But when $\lambda > D$, Q_{WW} can only be balanced by negative Q_{MF}. Negative Q_{MF} implies northward transport of PV by wave 1 which requires $q_1 < 0$ (section 2). The occurrence of positive wave–wave feedback depends on the generation of wave 1′ which requires $q_1 > 0$ for both waves 1 and 2. So the increase in wave–wave feedback for wave 1 is self-limiting in that it brings about negative values of Q_{MF} which are associated with $q_1 < 0$, and which lead to a reduction in the forcing of wave 1′. This explains the saturation noted in Fig. 4 for large amplitudes of wave 2.

b. Wave 2 in a wave 1 basic state

The behavior of small amplitude wave 1 in a wave 2 basic state is independent of the relative phases of the waves. However, when wave 2 occurs in a wave 1 basic state, the second meridional mode of the zonal flow, mode 0′, is generated, and this leads to a strong phase dependence for the results. The interaction between small amplitude wave 2 and finite amplitude wave 1 generates waves 3′, 1′, and 0′. The generation of wave 0′ depends on the phase lag between waves 1 and 1′ which in turn depends on the relative phases of waves 1 and 2. The presence of small amplitude wave 0′ does not affect the constancy of $\bar{q}_y/\bar{u}$ in the basic state.

Figure 6 shows the streamfunction at 32.5 km for a wave 1 basic state. Here wave 1 has a maximum geopotential amplitude of 1000 m at 47.5 km, a large but not unrealistic value (Geller et al., 1983). Of note are the regions of weak flow at 70°N, 150°W and 50°N,

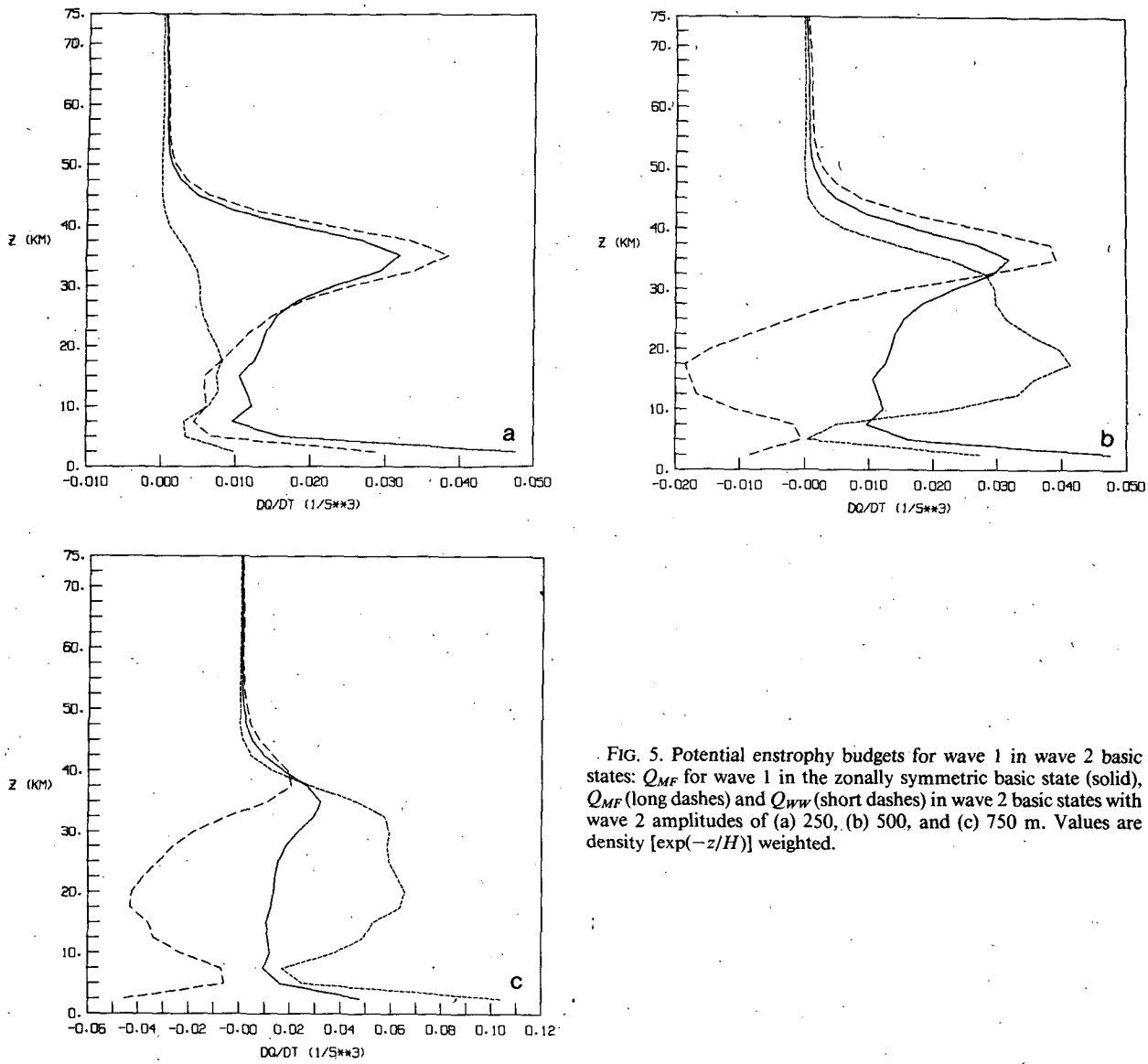

FIG. 5. Potential enstrophy budgets for wave 1 in wave 2 basic states: Q_{MF} for wave 1 in the zonally symmetric basic state (solid), Q_{MF} (long dashes) and Q_{WW} (short dashes) in wave 2 basic states with wave 2 amplitudes of (a) 250, (b) 500, and (c) 750 m. Values are density [$\exp(-z/H)$] weighted.

30°E, which are also regions of weak gradients in the basic state PV (not shown).

That wave 2 avoids these regions is demonstrated in Fig. 7. The perturbation streamfunction at 32.5 km is shown for wave 2 forced at 5 different phases. The phase of wave 2 relative to wave 1, $\Delta\Theta$, is given by

$$\Delta\Theta = 2\Theta_\psi(1) - \Theta_\psi(2). \quad (24)$$

When $\Delta\Theta = 0$, the ridges of wave 2 coincide with the ridge and trough of wave 1. The perturbation streamfunctions shown in Fig. 7 correspond to $\Delta\Theta$ equal to 0, 45, 90, 135, and 180 deg at 32.5 km. Wave 1 has the greatest effect on wave 2 when $\Delta\Theta$ is 0 or 180 deg. At these relative phases linear wave 2 would have its largest PV adjacent to the regions of weak flow and gradients of PV in the wave 1 basic state. These extrema of wave 2 are distorted and displaced meridionally away from the regions of weak flow. At $\Delta\Theta = 90$ deg the presence of wave 1 in the basic state has little effect on wave 2. The pattern in Fig. 7c is only slightly distorted from the perturbation streamfunction of wave 2 in a zonally symmetric basic state.

The perturbation streamfunctions are weakened as well as distorted by the interaction with wave 1. At $\Delta\Theta$ equal to 0 or 180 deg the presence of wave 1 constricts the width of the region in which wave 2 can propagate. The effective meridional scale of wave 2 is reduced. This traps wave 2 in the lower stratosphere below the heights at which wave 1 achieves large amplitudes. Figure 8 shows the amplitude of wave 2 for $\Delta\Theta$ equal to 0, 45, 90, and 135 deg. Wave 2 is severely trapped when $\Delta\Theta = 0$, while for $\Delta\Theta = 90$ deg the structure of

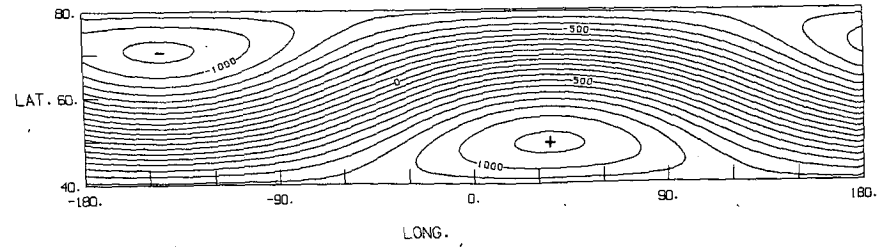

FIG. 6. Geopotential at $z = 32.5$ km for a wave 1 basic state. The contour interval is 100 m. Values are deviations from the mean geopotential height at this level. Geopotential highs and lows are denoted by plus and minus signs.

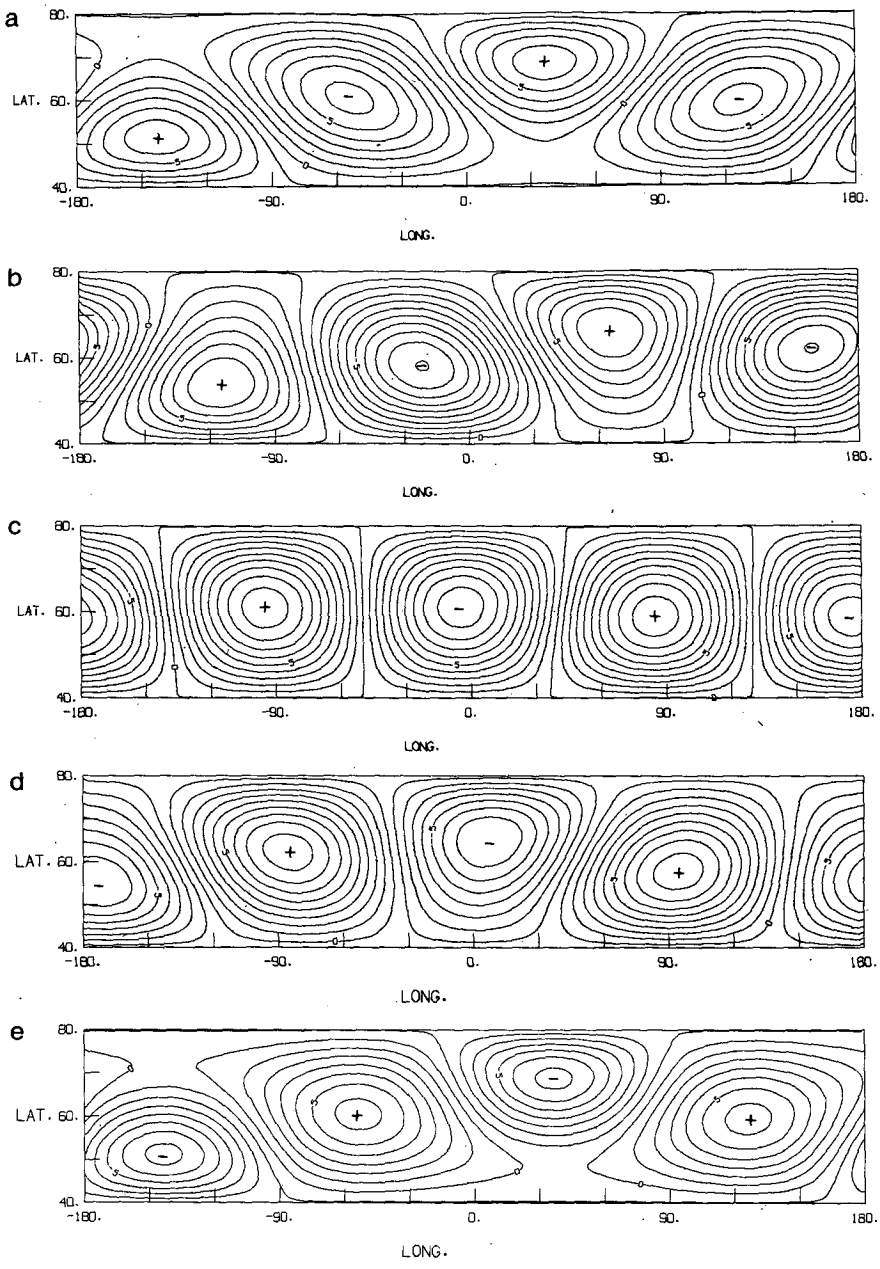

FIG. 7. Streamfunctions at $z = 32.5$ km for wave 2 disturbances in the wave 1 basic state. $\Delta\Theta$ = (a) 0, (b) 45, (c) 90, (d) 135, and (e) 180 deg. Highs and lows are denoted by plus and minus signs.

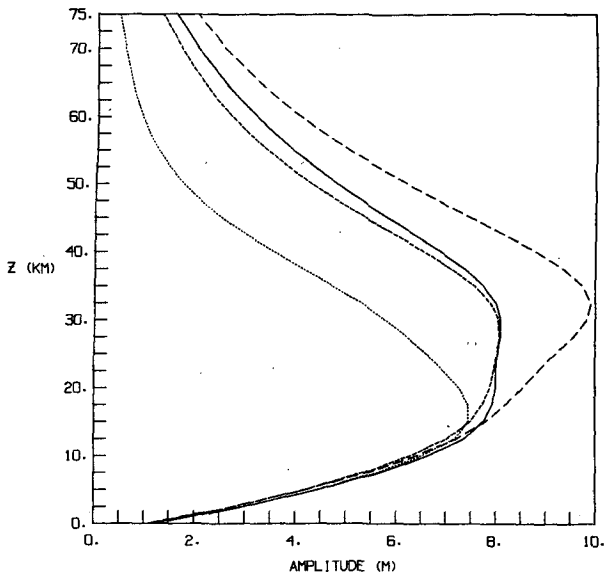

FIG. 8. Amplitudes of wave 2 in the wave 1 basic state at $\Delta\Theta = 0$ (dots), 45 (solid), 90 (long dashes), and 135 deg (short dashes).

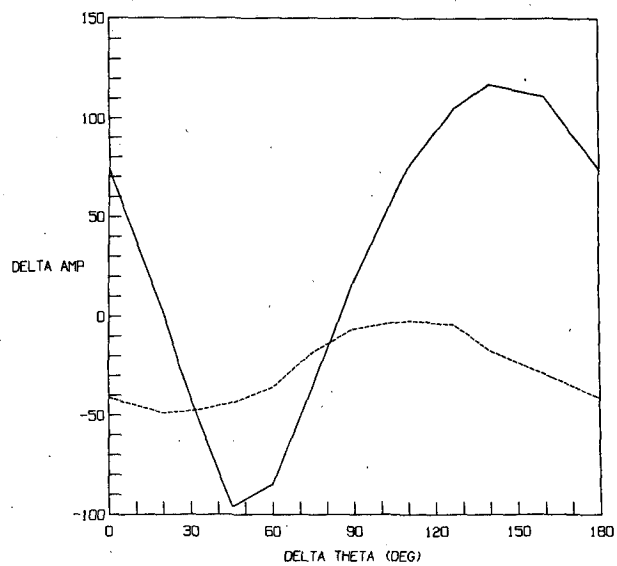

FIG. 9. Deviations of the geopotential amplitudes (m) of waves 1 (solid) and 2 (dashes) from their linear values as a function of $\Delta\Theta$ at $z = 32.5$ km.

wave 2 is indistinguishable from that shown in Fig. 3a for a zonally symmetric basic state.

5. Finite amplitude results

The experiments of the previous section are repeated allowing both waves 1 and 2 to vary in response to their interaction. Waves 1 and 2 are forced so as to have maximum geopotential amplitudes of 750 m and 250 m, respectively, in a zonally symmetric basic state. Figure 9 shows the deviations of the amplitudes of waves 1 and 2 from their linear values at 32.5 km as a function of the linear (initial) value of $\Delta\Theta$. The curves reflect a tendency for wave 1 to amplify and wave 2 to weaken as a consequence of their interaction. This is consistent with the behavior of wave 1 in a wave 2 basic state. However, the strong dependence of the results on $\Delta\Theta$ more resembles the behavior of wave 2 in a wave 1 basic state. This combination of results from section 4 is again evident in Fig. 10, which shows Q_{WW} at the same level for both waves. For most values of $\Delta\Theta$ PE flows out of wave 2 and into wave 1. These fluxes are nearly equal and opposite, indicating that while other waves act as conduits for the transfer of PE between waves 1 and 2, little PE is dissipated by these other modes.

That wave 1′ is responsible for these transfers of PE is shown in Fig. 11. The quantity $\Theta_\psi(1') + \Theta_\psi(1) - \Theta_\psi(2)$ is plotted against $\Delta\Theta$. From Eqs. 12 and 13 we see that wave 1 is reinforced for values between 0 and 180 deg, while wave 2 is reinforced for values in the lower half-plane. Comparing Fig. 10 with Fig. 11 shows that this is indeed what happens. For $\Delta\Theta$ between 40 and 100 deg, wave 2 gains PE from wave 1, while for other values of $\Delta\Theta$ wave 2 loses PE to wave 1.

Comparing Figs. 9 and 10 shows that the largest amplitudes of wave 1 are associated with those values of $\Delta\Theta$ at which Q_{WW} for wave 1 is largest, but that this is not the case for wave 2. For a stationary wave with zonal wavenumber k, in a constant zonal flow subject to weak equal rates D, of Newtonian cooling and Rayleigh friction and wave–wave feedback λ, the vertical structure is given by

$$\psi \sim e^{z/2H} e^{inz},$$

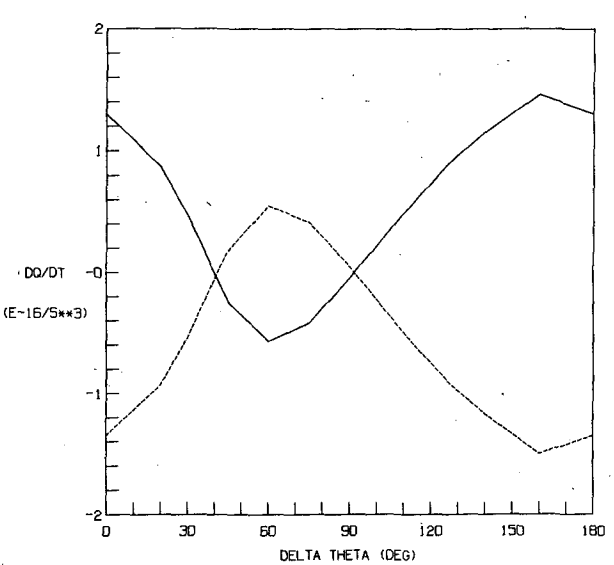

FIG. 10. As in Fig. 9 but Q_{WW} (10^{-16} s^{-3}).

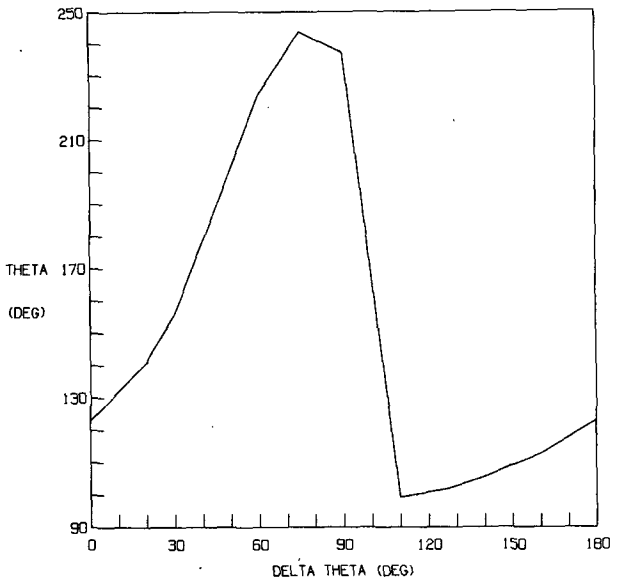

FIG. 11. $\Theta_\psi(1') + \Theta_\psi(1) - \Theta_\psi(2)$ at $z = 32.5$ km as a function of $\Delta\Theta$.

where n, the index of refraction, is given, to first order in the dissipation and feedback, by

$$n \approx n_0\left(1 + \frac{i}{2\epsilon n_0^2}\frac{\bar{q}_y}{\bar{u}}\frac{(D-\lambda)}{k\bar{u}}\right), \qquad (25)$$

where n_0 is the index of refraction in the absence of wave–wave interactions or dissipation:

$$n_0^2 = \left\{\epsilon^{-1}\left[\bar{q}_y/\bar{u} - \left(\frac{\epsilon}{4H^2} + K^2\right)\right]\right\}.$$

For a wave that is propagating vertically, n_0 is real, and increasing λ decreases the imaginary part of n and increases the growth of the wave's amplitude with height. For an evanescent wave, n_0 is imaginary, and increasing λ decreases the real part of n and reduces the wave's westward slope with height. This explains why waves 1 and 2 respond differently to changes in Q_{WW}. Consideration of the values of n_0 for waves 1 and 2 (not shown) indicates that linear wave 2 is evanescent above 15 km while linear wave 1 propagates up to 35 km.

Figure 12 is another illustration of how the nonlinear results combine the behavior of small amplitude wave 1 in a wave 2 basic state with that of small amplitude wave 2 in a wave 1 basic state. The vertical structure of Q_{WW} for wave 1 is shown for $\Delta\Theta$ equal to 20, 60, 90, and 140 deg. In all four cases Q_{WW} is positive below 15 km, in a region where wave 2 is stronger than wave 1. Aloft, where wave 1 is stronger, the results show the phase dependence characteristic of the results for small amplitude wave 2.

6. Conclusions

In summary we find that in a mean flow with horizontally constant $\bar{q}_y/\bar{u}$, interactions between stationary quasi-geostrophic waves occur entirely as a consequence of dissipation. The presence of dissipation induces a component of a wave's PV which is in quadrature with its streamfunction, and this component is responsible for interactions with other waves. The interactions are mediated by smaller scale waves that have horizontal wavenumbers too large to permit vertical propagation and that exist only because of interactions between vertically propagating modes.

Numerical experiments in a beta-channel indicate that small amplitude wave 1 is amplified by its interaction with finite amplitude wave 2. Because interactions with the mean flow tend to oppose the effects of wave–wave interactions, the amplitude of wave 1 is less sensitive to interactions with wave 2 than is the dynamical balance which maintains the wave. Small amplitude wave 2 is vertically trapped by its interaction with finite amplitude wave 1 when the ridges or troughs of wave 2 coincide with the ridge or trough of wave 1. When the extrema of wave 1 lie in between the extrema of wave 2, wave 2 is nearly unaffected by the presence of wave 1 in the basic state. When both waves possess finite amplitudes there is a tendency for wave 1 to gain PE at the expense of wave 2, but the results depend strongly on the relative phases of the waves, especially in the middle to upper stratosphere where wave 1 is dominant.

The climatological orientation of waves 1 and 2 in the stratosphere (van Loon et al., 1973) is such that their ridges coincide near the international date line, forming the Aleutian high. The present results suggest that with this orientation wave 2 should be trapped in the lower stratosphere when wave 1 is strong. It is reasonable to question the relevance of this effect to the

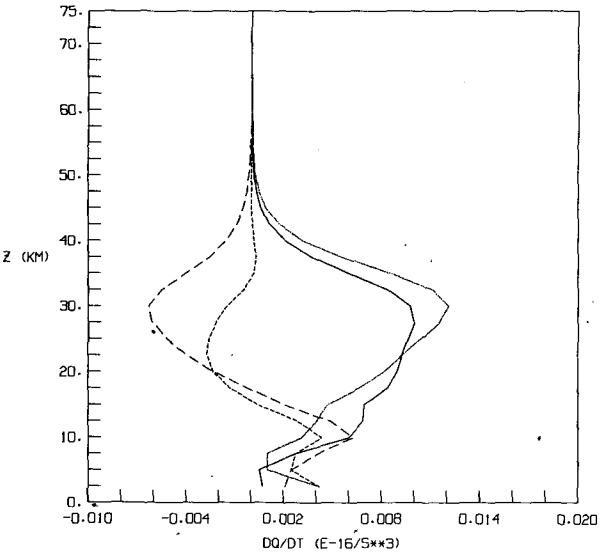

FIG. 12. Q_{WW} (10^{-16} s^{-3}) for wave 1 interacting with wave 2 with $\Delta\Theta$ = 20 (solid), 60 (long dashes), 90 (short dashes) and 140 deg (dots).

atmosphere where there are no rigid zonal boundaries. Observations of wintertime stratospheric flows (e.g., Ebdon, 1977) indicate that the polar night jet narrows where it passes between the Aleutian high and the pole. Waves propagating into this region will have their meridional scales reduced, possibly leading to vertical trapping like that which occurs for wave 2 in the present model. This could explain the observed weakness of wave 2 during periods in which wave 1 is very strong.

When wave 1 is relatively weak the model indicates that the interaction of wave 1 with wave 2 leads primarily to an amplification of wave 1. This is consistent with the generation of wave 1 by wave–wave interactions during December 1980, which was demonstrated by Austin and Palmer (1984). During this month wave 2 was more than twice as strong as climatology in the upper stratosphere (Geller et al., 1983). Austin and Palmer's primitive equation model reproduces the observed stratospheric amplitude of wave 1 when there is no wave 1 forcing at the lower boundary (100 mb) but interactions with other waves are included. In a simulation that includes wave 1 forcing but excludes wave–wave interactions the stratospheric amplitude of wave 1 is underestimated by nearly a factor of two.

Because they use the observed time dependent 100-mb geopotential to force their model, it is not possible to isolate the mechanism for the wave–wave interactions in Austin and Palmer's results. However, the present work suggests that such interactions could result from dissipation. Since all meridional scales of wave 1 are removed from Austin and Palmer's simulation, wave 3 must have mediated their wave–wave interactions, as opposed to the higher meridional mode of wave 1, which couples waves 1 and 2 in the present model.

Any results obtained with a severely truncated model are subject to the question of to what extent are the results an artifact of the truncation. A definite answer to this question can only be obtained by resorting to a model with many more degrees of freedom, for which the results will be harder to interpret. The truncation can be justified rigorously in the limit of small wave amplitudes and weak wave–wave interactions, assuming no resonant modes are generated. As the strength of the zonal asymmetries in the basic states described above are reduced, the wave–wave interactions are reduced in magnitude, but they do not change qualitatively. Nor are the results fundamentally altered by the exclusion of waves 3 and 3'. Thus, as a minimum, the present results represent the first order effects of wave–wave interactions on the structures of stationary waves.

While the simplicity of the present model does not allow detailed comparisons with observations or with the results of more comprehensive simulations, the results show that dissipation alone can induce interactions between stationary waves which significantly modify their structures. In the atmosphere zonal wave propagation, wave transience, and meridional variations in $\bar{q}_y/\bar{u}$ will also cause wave–wave interactions to occur. Here we have isolated one mechanism by which waves interact and shown that it can explain some of the behavior of stationary planetary waves which deviates from the results of linear theory.

Acknowledgments. This work formed part of the author's doctoral dissertation for the Department of Geological Sciences of Columbia University. The work was conducted at the NASA Goddard Space Flight Center/Institute for Space Studies. The preparation of this paper was supported under NASA Grant NAGW-662.

REFERENCES

Austin, J., and T. N. Palmer, 1984: The importance of nonlinear wave processes in a quiescent winter stratosphere. *Quart. J. Roy. Meteor. Soc.*, **110,** 289–301.

Charney, J. G., and P. G. Drazin, 1961: Propagation of planetary-scale disturbances from the lower into the upper atmosphere. *J. Geophys. Res.*, **66,** 83–109.

Derome, J., 1984: On quasi-geostrophic, finite amplitude disturbances forced by topography and diabatic heating. *Tellus,* **36A,** 313–319.

Ebdon, R. A., 1977: Average temperatures, contour heights and winds at 30 millibars over the Northern Hemisphere. *Geophys. Mem.*, **17,** 170 pp.

Geller, M. A., M.-F. Wu and M. E. Gelman, 1983: Troposphere-stratosphere (surface-55 km) monthly winter general circulation statistics for the Northern Hemisphere—four year averages. *J. Atmos. Sci.*, **40,** 1334–1352.

——, and W. M. Wehrbein, 1980: A numerical model of the zonal mean circulation of the middle atmosphere. *Pure Appl. Geophys.*, **118,** 284–306.

Holton, J. R., and C. Mass, 1976: Stratospheric vacillation cycles. *J. Atmos. Sci.*, **33,** 2218–2225.

Labitzke, K., 1977: Interannual variability of the winter stratosphere in the Northern Hemisphere. *Mon. Wea. Rev.*, **105,** 762–770.

Lin, B.-D., 1982: The behavior of winter stationary planetary waves forced by topography and diabatic heating. *J. Atmos. Sci.*, **39,** 1206–1226.

Matsuno, T., 1970: Vertical propagation of stationary planetary waves in the winter Northern Hemisphere. *J. Atmos. Sci.*, **27,** 871–883.

Schoeberl, M. R., and M. A. Geller, 1977: A calculation of the structure of stationary planetary waves in winter. *J. Atmos. Sci.*, **34,** 1235–1255.

Simmons, A. J., 1974: Planetary-scale disturbances in the polar winter stratosphere. *Quart. J. Roy. Meteor. Soc.*, **100,** 76–108.

Smith, A. K., 1983: Observation of wave–wave interactions in the stratosphere. *J. Atmos. Sci.*, **40,** 2484–2496.

——, J. C. Gille and L. V. Lyjak, 1984: Wave–wave interactions in the stratosphere: Observations during quiet and active wintertime periods. *J. Atmos. Sci.*, **41,** 363–373.

Tung, K. K., 1983: On the nonlinear versus linear lower boundary conditions for topographically forced stationary long waves. *Mon. Wea. Rev.*, **111,** 60–66.

van Loon, H., R. L. Jenne and K. Labitzke, 1973: Zonal harmonic standing waves. *J. Geophys. Res.*, **78,** 4463–4471.